1. Introduction

For this stage I am involved in the research work on the DAFNE experiment. The main goal of this experiment is to test new ideas which proposed for building a superb-factories, which should run at a luminosity 100 times higher than the one at the present facilities. My job is to simulate the geometry of the interaction region of the DAFNE experiment (and in particular of the detectors devoted to the measurements of the luminosity). An important aspect of my work will concern the characterization of the machine background. The work and the expertise acquired in these studies will be than transferred to the superb-factory environment, project I'll be involved for my PHD-thesis.

Here in the following a schematic introduction of the different chapters this report consists of.

In section 1 I'll discuss the Standard Model with particular attention for the fermion sector and thus the CKM matrix. I'll introduce the CP violation and I show the role of the B physics and from experimental point of view of the B-Factories facilities. In section 2 (State of the art in the B-physics) I briefly discuss about physics motivations to explicitly show why it is important to study B-physics precisely, and thus to construct a SuperB-factory. Before going specifically to the work foreseen for my "stage" and my thesis I'll briefly introduce the group I'm working with.

In section 4 (How to build super-B factory) I'll discuss the new ideas of accelerating schemes which would allow to reach a luminosity of about a factor 100 better than the present B-factory luminosity. I'll show how these new schemes have been implemented in the new interaction region of DAFNE.

1.1 The Standard model of the elementary particle

Standard model (SM) of the particle physics is able to describe all the observations to date. The role of this model is to establish and group in families the list of the all the existing elementary particles and to describe their interactions. The table below gives a summary of the 12 fermions (6 quarks and 6 leptons) and their main characteristics. These particles are classified in three generations. The higher the generation the heavier the particle is.

Table1.1 *of particle and their main characteristics*

Particle	**Where we find it ?**	**Discovery**	**charge**	**Mass**
QUARKS	HADRONS	1905-1995	-1/3-2/3	2Mev-176GeV
up-down *(u,d)*	proton –neutron	Proton(1905) Neutron (1932)	up 2/3 down -1/3	~2-4 MeV
strange *(s)*	particules étranges(K,Λ..)	Kaons(1947)	-1/3	~100MeV
charm *(c)*	Hadrons D, J/Ψ	J/Ψ (1975)	2/3	~1.4GeV
beau *(b)*	Hadrons B	Upsilon(1977)	-1/3	~5.2 GeV
top *(t)*		top(1995)	2/3	176GeV
LETPONS		1898-2000	0,-1	~0-1784MeV
electron *(e)*		1898	-1	0.5MeV
neutrino e *(ν_e)*		1956	0	~0
muon *(μ)*		1937	-1	106.5MeV

neutrino mu (ν_m)		1962	0	~0
tau (τ)		1975	-1	1784MeV
neutrino tau (ν_t)		2000	0	~0

Observation of the symmetries can help to build theory of the interaction. For example, observation that the electric charge of system is invariant in an electromagnetic process indicates that the lagrangian describing the electromagnetic interaction has to be invariant under the U(1) gauge transformation. Similarly, the Standard Model (SM) is based on the observation that a quantum number named "colour" is conserved in strong interaction while the electroweak interaction conserve the "weak isospin" and "hypercharge" quantum numbers. The corresponding jauge group is $SU(3)_c \times SU(2)_L \times U(1)_Y$. The interactions are vehiculated by particles with spin 1, the bosons : for the electromagnetic interaction, the photon, three gauge bosons for the weak interaction: W^+ , W^- and Z^0, eight gauge bosons for the strong interactions, the gluons. Experimentally W^+, W^- and Z^0 bosons have been observed to have non zero masses. These masses are explained in the theory thanks to the presence of the Higgs field and the spontaneous symmetry breaking mechanism. The values of the masses are not predicted by the SM, and have to be measured. The large difference between the values obtained for the first and the last generation are not explained by the model.

1.2 Symmetry

As it was mentioned above symmetries are very important in physics, since they establish relations within quantities in principle uncorrelated. In a field theory described by a Lagrangian (L), a transformation is symmetry of the theory if L does not change under the transformation.

The parity transformation change the x coordinates of the physical system into their opposite. It affect the momentum p , but leaves unchanged the spin of a particle, so that the helicity is also changed in to the opposite.

$$x \rightarrow -x$$
$$p \rightarrow -p$$
$$h \rightarrow -h$$

Somehow it creates the mirror image of the physical system. Parity symmetry is valid if the result of the parity transformation of a system is a system that indeed exists in nature, with the same probability.

Parity symmetry appears to be valid for all reactions involving electromagnetism and strong interactions. Until 1956, parity conservation was believed to be one of the fundamental conservation laws (along with conservation of energy and conservation of momentum). However, it is violated in week interaction, neutrinos, which can interact and be created only thought weak interaction processes, exist only as left-handed particle ($\nu_L; h = -1$). The parity transformation applied to this particle leads to a right-hand neutrino ($\nu_R; h = 1$) that does not exist in nature (see fig1.2.1).

The charge conjugation operator C change the charge of a particle into their opposite. For most of the particles, charge conjugation is equivalent to change them into their associated anti particle (see fig1.2.1). If we use again the example of neutrinos we see that a left-handed neutrino would be transformed by C into a left-handed anti-neutrino which does not exist in nature. This is a manifestation of the C symmetry violation in weak interaction.

	Exist	Not exist
C	$\nu_L \rightarrow$	$\bar{\nu}_L$
P	$\nu_L \rightarrow$	ν_R

Figure1.2.1 *Result action of the P and C operators separate*

	Exist	Exist
CP	$\nu_L \rightarrow$	$\bar{\nu}_R$

Figure1.2.2 *Result action of the P and C operators together*

Those are discrete symmetries that can be combined, for example the operation CP changes a particle in its antiparticle and inverts its momentum and helicity (see fig1.2.2). It was proposed in 1957 by Lev Landau as the true symmetry between matter and antimatter. The CP violation of the weak interactions has been observed for the first time in 1964 in the study of rare decays in the neutral kaon system and recently observed also in B mesons decays, thanks to the data collected by the B-factory experiments. On the other hands the transformation CPT must be symmetry for every local field theory and it is confirmed to be conserved by all experimental searches up to now.

1.3 Flavour Physics: CKM Matrix and CP violation

The "natural choice" was to use the quark flavour eigenstates basis. In this basis the 3x3 mass matrices are complex and only quarks of the same family can communicate. The choice of operating in the quark mass eigenstates basis has the advantage of reducing the mass matrices to be real and diagonal with eigenvalues corresponding to the quarks masses. It has also the important consequence to of moving the quark mixing (and CP violation) from the mass sector to the electroweak Lagrangian sector, where it is described by the quark mixing matrix called Cabibbo-Kobayashi-Maskawa (CKM)-matrix:

$$\begin{pmatrix} d' \\ s' \\ b' \end{pmatrix}_f = \begin{pmatrix} V_{ud} & V_{us} & V_{ub} \\ V_{cd} & V_{cs} & V_{cb} \\ V_{td} & V_{ts} & V_{tb} \end{pmatrix} \times \begin{pmatrix} d \\ s \\ b \end{pmatrix}_m \tag{1.3.1}$$

In a sense this matrix specifies the mismatch between quantum sates of quarks when they propagate freely (mass eigenstates). The elements $|V_{q_1 q_2}|^2$ rule the probability of the $q_2 \to q_1$ transition. Being the CKM matrix a 3 X 3 matrix, it can always be parametrized with three Euler angles (real parameters) and six phases (complex parameters). Five of these six phases disappear under transformations that redefine the phase of the quark fields in the quark mass eigenstate basis and leave the diagonal mass matrix unchanged. One of the six phases is irreducible. The presence of this phase accounts for the CP violation in the Standard Model.

Many parameterizations for CKM matrix have been proposed, one of them is Wolfenstein parameterization. Starting from the consideration that the mixing angles are small, the Wolfenstein parametrization emphasizes a hierarchy in the magnitudes of the CKM elements: the ones on the diagonal are of order 1, and the others become smaller the more they are far from the diagonal. In the Wolfenstein parametrization, the matrix elements are the result of an expansion in terms of a small parameter $\lambda = |V_{us}| \sim 0.22$. The four independent parameters are in this case: λ, A, ρ, η, where η is the CP violating phase and the matrix is written, to order λ^3:

$$\begin{pmatrix} 1 - \frac{\lambda^2}{2} & \lambda & A\lambda^3(\rho - i\eta) \\ -\lambda & 1 - \frac{\lambda^2}{2} & A\lambda^2 \\ A\lambda^3(1 - \rho - i\eta) & -A\lambda^2 & 1 \end{pmatrix} \tag{1.3.2}$$

1.4 The Unitarity Triangle

The CKM matrix has a property known as unitarity $V \cdot V^+ = 1$. Mathematically, this defines a set of equations that the matrix elements must satisfy. In practice it implies several relations between its elements and in particular six independent vanishing relations (triangular relations). Each one of these

relations can be represented as a triangle in the (ρ–η) plane. Within the six relations, we choose one such equations:

$$V_{ud}V_{ud}^{*} + V_{cd}V_{cd}^{*} + V_{td}V_{td}^{*} = 0 \qquad (1.4.1)$$

Whose elements can be determined by B physics measurements. This triangle is particularly attracting from the experimental point of view, since it has all the sides of order λ^3.We obtain an equivalent equation if we divide both sides of the equation by the middle term:

$$\frac{V_{ud}V_{ud}^{*}}{V_{cd}V_{cd}^{*}} + 1 + \frac{V_{td}V_{td}^{*}}{V_{ud}V_{ud}^{*}} = 0 \qquad (1.4.2)$$

Complex numbers can be represented as points on a two dimensional plane, or equivalently as vectors in a plane. Each term in the above equation is complex and can be drawn as a vector in the plane.

The imaginary coordinate of the apex is η the CP violating phase and, as already stated, the presence of CP violation, i.e. η different from zero, is described by the area of the triangle being non-vanishing.

The angles and the sides of the Unitarity Triangle, or quantities strictly related to them, are accessible by different experimental techniques.

The main goal of this activity is to try to have evidence of New Physics beyond the Standard Model. One possibility of getting that is to measure the sides and the angles of the Unitarity Triangle in many different independent ways and with very good precision. In fact deviations from the triangle shape are an indication that the SM is not able to coherently describe all the phenomena and thus a signature for New Physics.

1.5 B-factories

In the last decade the main actor of B physics have been played by the B-factories.

BaBar experiment at the PEP2 at the Stanford Linear Accelerator Center (SLAC) and the Belle Experiment at the High Energy Accelerator Research Organisation (KEK) in Japan, produced $\sim 10^9$ $B, \overline{B}$ pairs.

(il faut ecrire plus…)

2. State of the art in the B-physics

In B-mesons decays there are many observables that give access of the unitarity triangle. B-factories have recently performed several measurements of the sides and of the angles. In figure 1 we show the allowed regions for ρ and η as given by all the available measurements.

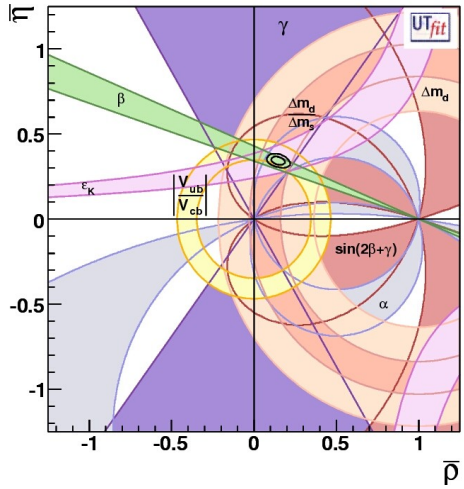

Figure2.1 *Allowed regions for ρ–η, as given by the measurement sides and angles ($|V_{ub}|/|V_{cb}|$, Δm_d , Δm_s ε_K α, β, γ, 2β+γ, cos2β). The closed contours show the 68% and 95% probability regions for the triangle apex, while the colored zones are the 95% probability regions for each constraint. The experimental values are updated using results presented at the 2008 winter conferences.*

As a general fact, as it can be seen in figure2.1 the Standard Model description of CP violation through the CKM mechanism appears as a very successful framework, able to account for all the measured observables up to the actual precision. In this situation, any effect from physics beyond the Standard Model should appear as a correction to the CKM picture.

To be able to look for NP the precision of the measurements have to be improved substantially. Without going into the details, we show the potentiality of a Superb-factory capable to collect 100 times the statistics actually available at the B-factory.

In Figure 2 we show the regions on the ρ–η plane selected by different constraints assuming the current measurement precision, and that expected at the SuperB factory. With the precision reached at SuperB, the current agreement.will not appear anymore such that but as a clear discrepancy indicating the presence of NP in the flavour sector.

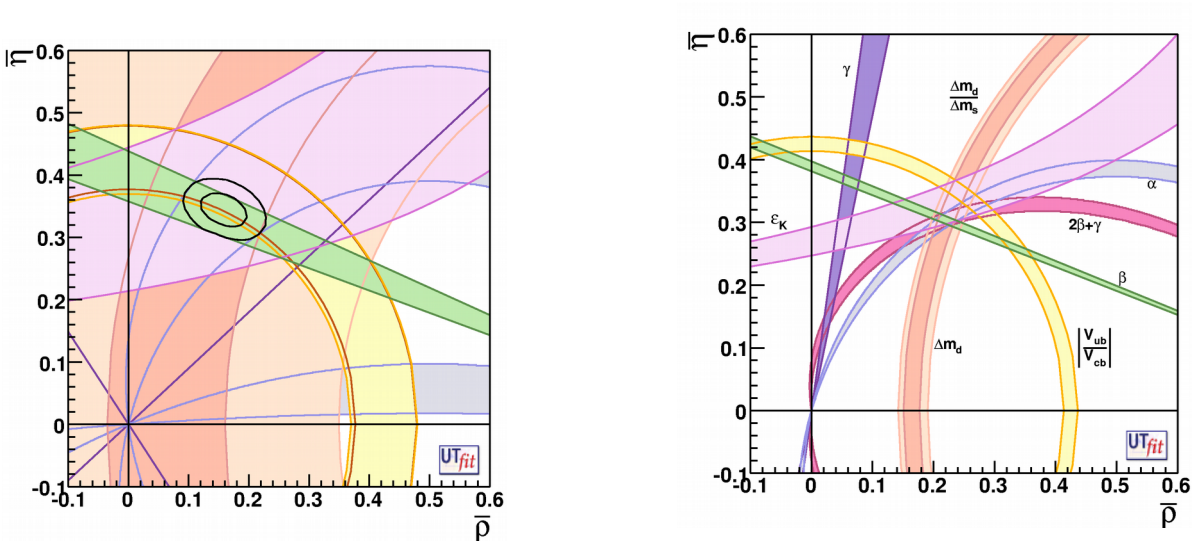

Figure2.1 *Regions corresponding to 95% probability for ρ and η selected by different constraints, assuming present central values with present errors (left) or with errors expected at SuperB (right).*

Another way for looking for New Physics is to measure the same quantity in different ways, namely using different processes which can be differently affected by the presence of new physics. We give here just one example. The angle β can be measured from B_d decay:

$$B_d \to J/\psi K_s^0 \tag{2.1}$$

The final state can be reached in two different ways as shown in fig.2.2 and 2.3. B^0 can decay directly to the final state or first oscillate into its antiparticle $\overline{B}^0$ and than decay.

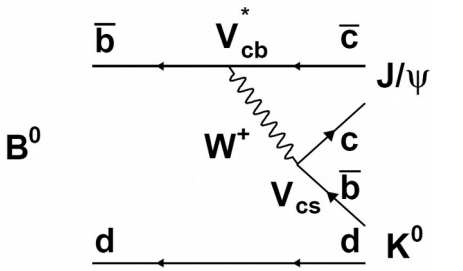

Figure2.2 *Decay of the B-meson into J/ψ and K_s^0.*

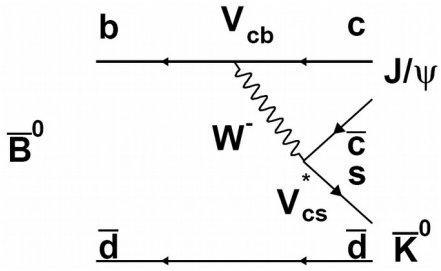

Figure2.3 *Decay of the B-meson into J/ψ and K_s^0.*

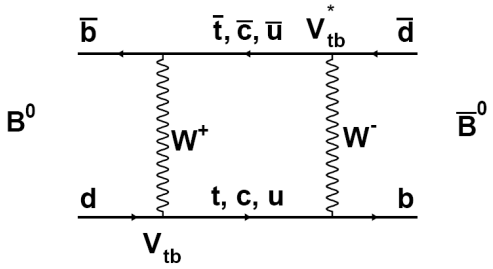

Figure2.4 *Oscillation of the of the B-meson.*

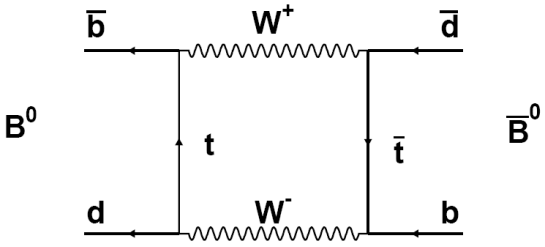

Figure2.5 *Another possibilities of the Oscillation B-meson.*

Oscillations are represented by two diagrams (see Fig.2.4 and 2.5). This process has been used to obtain the first CP violating quantity measured by the B-factories. It is now a precision measurement.

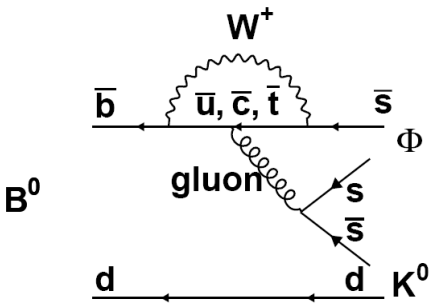

Figure2.6 *In this picture depicted Feynman diagram of the B0→ϕ K⁰ decay process.*

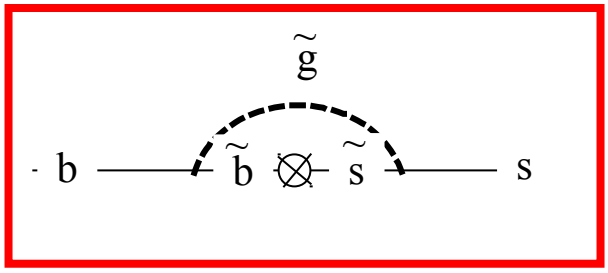

Figure2.7 *The transition b→s occurs via the exchange of Supersymmetric particles (gluino and squarks : sbottom and s-strange)*

On the other hands the angle β can be measured using the process (called Pinguins) indicated in Figure 2.6. Here the technique used is the same as for the previous mode. Nevertheless the value obtained for β can be affected by the presence of NP contributing to the final state ϕK^0 as indicated in Figure 2.7. The experimental situation is summarized in Figure 2.8. Some discrepancy between the values of β obtained from $B^0 \rightarrow J/\psi\ K^0$ and $B^0 \rightarrow \phi\ K^0$ (and related channel) is visible. The precision is not sufficient to state the presence of NP. In Figure 2.9 we show the expected errors on the "Pinguins" processes from a SuperB factory. The SuperB factory could see a deviation between the two determinations of β at a per cent level.

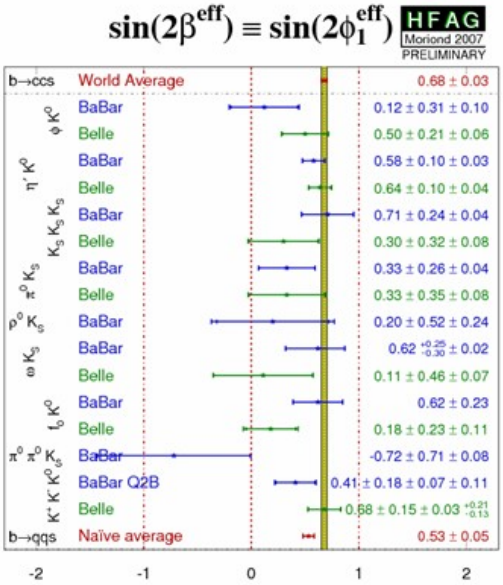

Figure2.8 *Present situation for the measurement of β obtained from $B^0 \rightarrow J/\psi\ K^0$ and $B^0 \rightarrow \phi\ K^0$ (and related channel).*

Observable	B Factories (2 ab^{-1})	Super$B$ (75 ab^{-1})
$S(\phi K^0)$	0.13	0.02 (*)
$S(\eta' K^0)$	0.05	0.01 (*)
$S(K^0_S K^0_S K^0_S)$	0.15	0.02 (*)
$S(K^0_S \pi^0)$	0.15	0.02 (*)
$S(\omega K^0_S)$	0.17	0.03 (*)
$S(f_0 K^0_S)$	0.12	0.02 (*)

Figure2.9 *The expected error for the measurement of S=sin2β for Pinguins mediated channel at a SuperB.*

3. Presentation of the laboratory and the team

A small group has been formed at LAL (**Laboratoire de l'accelérateur linéaire**) to work on the activities related to the SuperB factory project. This group is composed by N. Arnaud, A. Variola, A. Stocchi and B. Viaud. This group has been involved in several activities. The first activity has been the write up of the Conceptual Design Report (CDR). This document of 444 pages consists of three parts: Physics Case , Machine and Detector for the SuperB. One member of the LAL group (A. Stocchi) had the responsibility of co-convener of the part concerning the Physics Case. On the other hand A. Variola

followed closely the activities and contributes to the new ideas for the accelerating schemas. This document has been submitted to the expertise of an International Review Committee (IRC). After the CDR finished the activities about the Physics Case have been continued with the participation at few workshop. A document has been recently written, after the Valencia meeting (A. Stocchi and B. Viaud). This document was mainly intended to answer some questions raised from the IRC.

Finally in the last 9 months all the group has been involved in the activities on the upgrade of DAFNE to test the new schemas of acceleration, known as "crab waist scheme". The group took the responsibility of the simulation of the interaction region and in particular of the luminosity system. The group also assured an important presence in Frascati (N. Arnaud and B. Viaud) for the installation, the test beam and the commissioning of the luminomiters. A. Variola also participate to the running of the machine.

My work at LAL is under the supervision of Prof. Achille Stocchi and postdoctoral student Dr. Benoit Viaud.

4. How to build superB-factory.

We present in this section the main ideas proposed to build a B-factory able to produce 100 times more B-B pairs than the present B-factories. We also give a short introduction to the backgrounds produced by the beams of such a machine. This is an important aspect, impacting on the design of the accelerator and of the detectors to be installed at the interaction point to study B physics.

4.1. Luminosity

In general luminosity can be expressed thought next equation:

$$L = \frac{N_1 N_2 \times f}{2\pi\sigma_x\sigma_y\sqrt{1+\Phi^2}}, \tag{4.1}$$

Where N_1, N_2 are the number of particle in the e^- and e^+ bunches respectively, f is the frequency at which an electron bunches crosses positron bunch at the interaction point. Inside a bunch, the particles are distributed according to 3dimensional Gaussian. The horizontal and vertical variances of this Gaussian are $\sigma_x\sigma_y$, while the longitudinal variance σ_z is a bunch length. The Piwinski angle is given by equation (4.2).

$$\Phi = \frac{\sigma_z}{\sigma_x} tg(\frac{\theta}{2}), \tag{4.2}$$

where θ is the angle between the electron and positron beams (fig.4.2).

Luminosity can de increasing by changing different input values in (2) by various of possibility. One way consists on increasing the beam currents ie. f, N_1, N_2. However this option is very expensive.

Another way to impove the luminosity is to reduce σ_x and σ_y. This option is the one chosen by the Super B-factory project to which the LAL's group contributes [].

This option is tested at present moment at e^+/e^- collider at DAFNE accelerator in Frascati, Rome. A bunch is a group of electric charges. So it creates an electromagnetic field. When en electron (positron) bunch crosses positron (electron) bunch, it feels this field. This interaction can cause perturbation to the beams, that will make them harder to control. These effects are larger if the beams are more dense (large field) and if the bunches are larger (large interaction length). For example one such effect called disruption is expressed in the following way:

$$D \approx \frac{N\sigma_z}{(\sigma_x\sigma_y)} \tag{4.3}$$

Consequently if we reduce σ_x and σ_y, we also need in principle to reduce σ_z

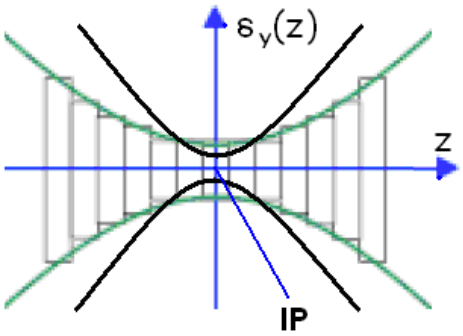

Fig.4.1 Vertical size $\sigma_y(z)$ of a bunch when it is crossing the Interaction Region. This profile results from the focalization of the beams.

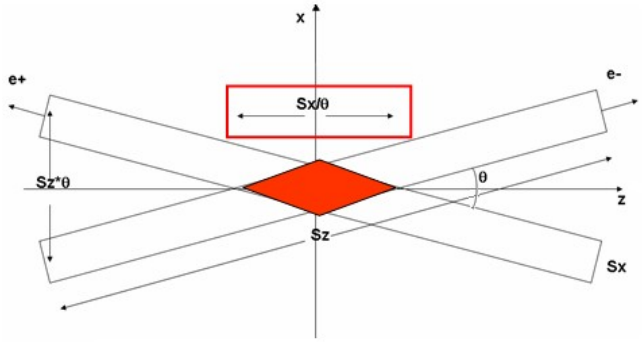

Fig.4.2. Two bunches colliding with a crossing angle. The red lozenge figures the new interaction region, now short enough to avoid excessive beam-beam interactions and hourglass effect.

This reduction would also help reducing the impact of the hourglass effect. A commonly used technique to improve the luminosity is to focus vertically the beams while they travel the last meter before the interaction point .This allows the particle density, thus the luminosity to be large at the IP. However the quicker the focalization when approaching the IP, the quicker the defocalization when leaving the IP. This can be seen on figure 4.1, which shows the profile of a bunch at the moment when it is centered at the IP. We can see that the vertical size σ_y is bigger at the head and the tail of the bunch, as is the particle density. As a result, if the bunch length is too large with respect to the speed of the focalization as a function of z, e^+/e^- collisions occurring away from the IP become so rare that the total luminosity will drop despite of the improvement obtained right at the IP. This hourglass effect disappears if σ_z is short enough so that all the collisions happen close to the IP, where the density is maximal.

Technical reasons too complicated to enter the scope of this document make it very hard to. shorten σ_z. This super-b project use an alternative approach: the beams collide with a crossing angle, the effective length of the interaction region is:

$$\sigma_z' = \sigma_x / \theta << \sigma_z \qquad (4.4)$$

Colliding with crossing angle introduces a new problem. As can be seen on figure 4.3 when an electron (for example) flies through the positron beam it sees a positron charge density that varies along its trajectory. It's due to the misalignment between the e^- trajectory and the direction of the $\sigma_y(z)$ focalization of the e^+ beam. Since it see longitudinal variation of the charge density. The magnetic field it feels also varies, as does the corresponding force. Thus, a coupling between the horizontal, vertical and longitudinal dynamics appears and is responsible for additional oscillation modes of the particle all around the accelerator. This increases the number of potential resonances and makes the beams harder to control. To solve this problem, sextuples are placed on both sides of the IP to tune the beam focalization in such a way that its maximum is reached earlier or later, according to the distance to the center of the beam in the horizontal plane. This crabbed waist scheme (fig.4.4) allows particles to see the same field all along their trajectory while crossing the positron bunch, and to avoid these additional resonances.

These ideas of using a crossing angle and crabbed waist have been designed using simulations. It is also necessary to test them experimentally. This is the goal of the test presently carried out at Frascati.

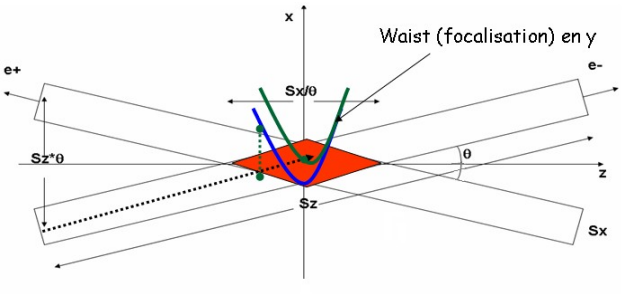

Fig.4.3 Bunch crossing with normal waists. When an electron flies through the positron beam, the charge density it meets varies as a function of its longitudinal position. This density variation can be intuited with the help of the green and blue lines, which represent the positron bunch vertical size.

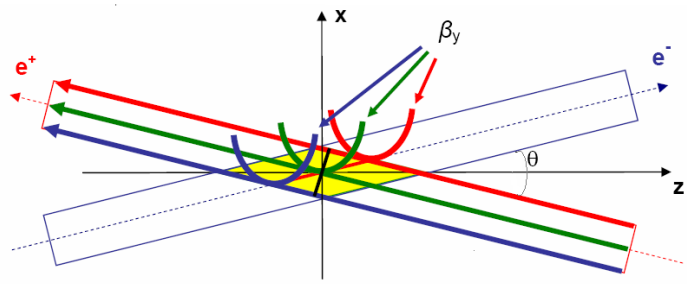

Fig.4.5 Bunch crossing with "Crabbed waist". The position of maximal vertical focalization for the positron bunch is a function of the distance to the longitudinal axis of this bunch. It is tune so that the electrons crossing the interaction region (yellow) feels the same magnetic field whatever their longitudinal position.

4.1. Backgrounds

The design of an accelerator is not guided only by the need of maximizing the luminosity. One also have to keep the "backgrounds" at an acceptable level. This background are made of the many particles that are produced directly or indirectly by the beams, and can cause damages to the physics detectors and make the the signals we want to study more difficult to identify.

There are many types of backgrounds. For instance, since the vacuum in the beampipe is never perfect, the electrons and positrons of the beams can collide with nuclei of the remnant gas. This produces many secondary particles that can hit the detector. Another example of background arises from the synchrotron photons emitted by a beam where its trajectory is curved.

Of particular interest is the "Touschek" background. This background is due to the scattering between particles inside the same bunch. The scattered particles can have their momentum modified enough to be lost by the beam and become a source of background. This effect is proportional to the density of particles in the bunch. Thus, the number of Touschek particles increases when the horizontal and vertical sizes of the bunch, σ_x and σ_y, are reduced. This will be one of the dominant sources of the background affecting a Super B-factory based on collisions with crossing angle and crabbed waist, since it uses very small transverse sizes to reach the aimed luminosity (10^{36} cm^{-2} s^{-1}). It is therefore important to understand this effect as precisely as possible.

5. Test of the crab waist scheme at the Frascati DAFNE accelerator complex.

The LNF Accelerator Division modified the DAFNE interaction region: the new layout is based on the "crabbed waist" scheme described in the previous section. The goal of this upgrade is to test if this new approach can indeed increase the collider luminosity by up to an order of magnitude. Although this measurement is by far the priority, one can also consider the opportunity to test the physics simulations that are used to describe the beam backgrounds that will affect a Super B-factory, by confronting their predictions in the context of DAFNE with measured data.

The Super B group at LAL has been working on the luminosity measurement for the last 9 months. The purpose of my internship is to extend its activities to the study of the backgrounds.

In this section, I briefly describe the upgrade of DAFNE. Then, although it is not the primary object of my work, I describe the luminosity measurement, since the background measurement I am

involved in uses the same detectors and is anyway influenced by the material distribution of the whole experimental set-up. Section 6 will deal with the background study in itself.

5.1 Upgrade of the DAFNE interaction region.

The initial purpose of the DAFNE is the study of kaon physics. It has been designed as a Φ-factory, providing as many kaon pairs as possible by colliding 510 MeV electrons and positrons to reach the Φ-resonance. An overview of this collider is shown on figure 5.5. A closer view of the interaction region is available on figure 5.6. This figure, in particular, shows how this region has been upgraded to test the crab waist scheme. Figure 5.1 shows the main beam parameters and the luminosity that should be obtained with this new set-up, compared to the best ones obtained before the upgrade. We expect the luminosity to be improved by a factor ~7. This would be the proof that crab waist scheme indeed works.

	DAΦNE KLOE	DAΦNE Upgrade
I_{bunch} (mA)	13	13
N_{bunch}	110	110
σ_y^* (μm)	7	2.6
σ_x^* (mm)	0.7	0.2
σ_z (mm)	25	20
$\theta_{cross}/2$ (mrad)	12.5	25
$\Phi_{Piwinski}$	0.45	2.5
L ($cm^{-2}s^{-1}$) x 10^{32}	1.5	10

Figure 5.1 Main accelerator parameters, before (left) and after (right) the upgrade.

5.2 Luminosity measurement

It is crucial to measure the luminosity produced with the new configuration of the DAFNE collider. For that purpose, a luminometer has been built, tested and installed at the DAFNE IP. It estimates the luminosity by reconstructing BhaBha scattering events: $e^+e^- \rightarrow e^+e^-$. This physics process is convenient for luminosity measurement because of its very clear experimental signature (two back-to-back tracks in the detector) that makes it easier to select the signal while rejecting backgrounds. Also, the probability to produce a BhaBha event in a given e^+/e^- collision is well known theoretically: it is a fairly "simple" electrodymamics process (fig. 5.1, top) that can be accurately evaluated via a perturbative calculation. Consequently, measuring the BhaBha production rate with the luminometer allows to derive precisely the initial number of the e^+/e^- collisions, thus the luminosity. Note that radiative Bhabhas, in which a photon is emitted by an electron or positron in the initial or final state, are also used.

The main parts of the detector are shown in the fig.5.1. It consists on 3 types of the detectors: calorimeters, gas electron multipliers (GEM) and low angle photon monitors. There are two detectors of each type, identical and placed at symmetric locations on both sides of the IP. The calorimeters

reconstruct the energy of the tracks produced in a BhaBha scattering event. The calorimeters are of cylindrical shape and placed transverse to the beampipe. Each calorimeter is made of 12 azimuthal sectors, of trapezoidal shape, which angular size equals 30° and is divided into 2 "modules", one above the beampipe, and the other below. Each sector is a sandwich of 12 scintillating plastic tiles and 11 lead layers, 1 cm thick. When an electron hits one lead layer, it decays in to a shower of many electrons and photons.

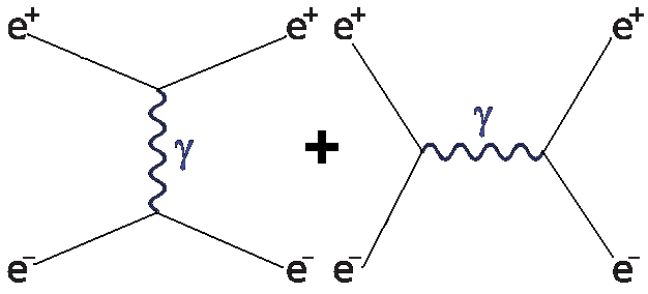

Figure.5.2 *Bhabha process.*

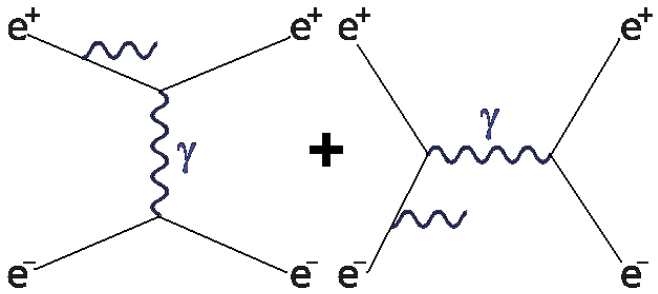

Figure.5.3 *Radiative Bhabha process.*

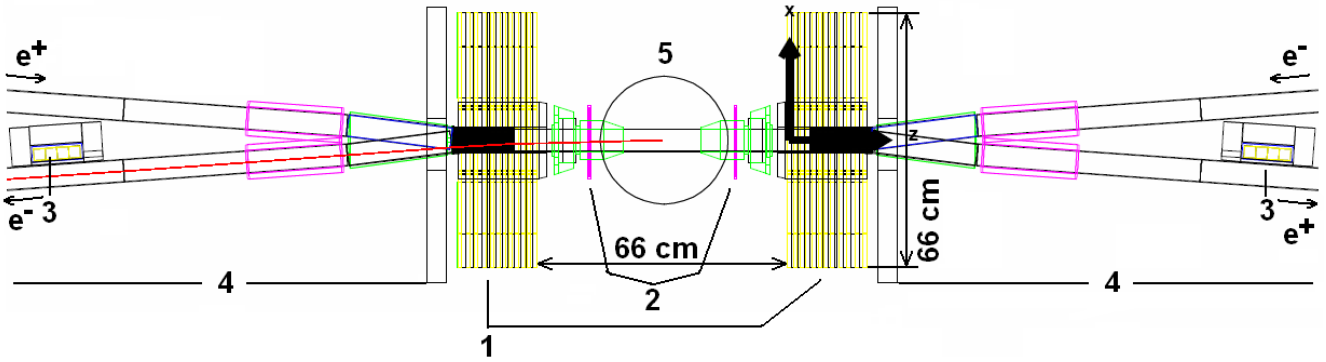

Figure.5.4 *Overall layout of the simulation seen from above. The positrons (electrons) travel along the +z (-z) axis, i.e from the left to the right (from the top to the bottom). The mail elements are: (1)-The two lead-scintillator calorimeters. (2)-The GEM trackers. (3)-The photon detector. (4)-The backward region where the two beams split. The pipe is surrounded by the QD0 QF1 magnets which goal is to tune the crossing angle and to focus the bunch in the IP region (QD0). (5)-A conical volume representing the SIDDHARTA detector.*

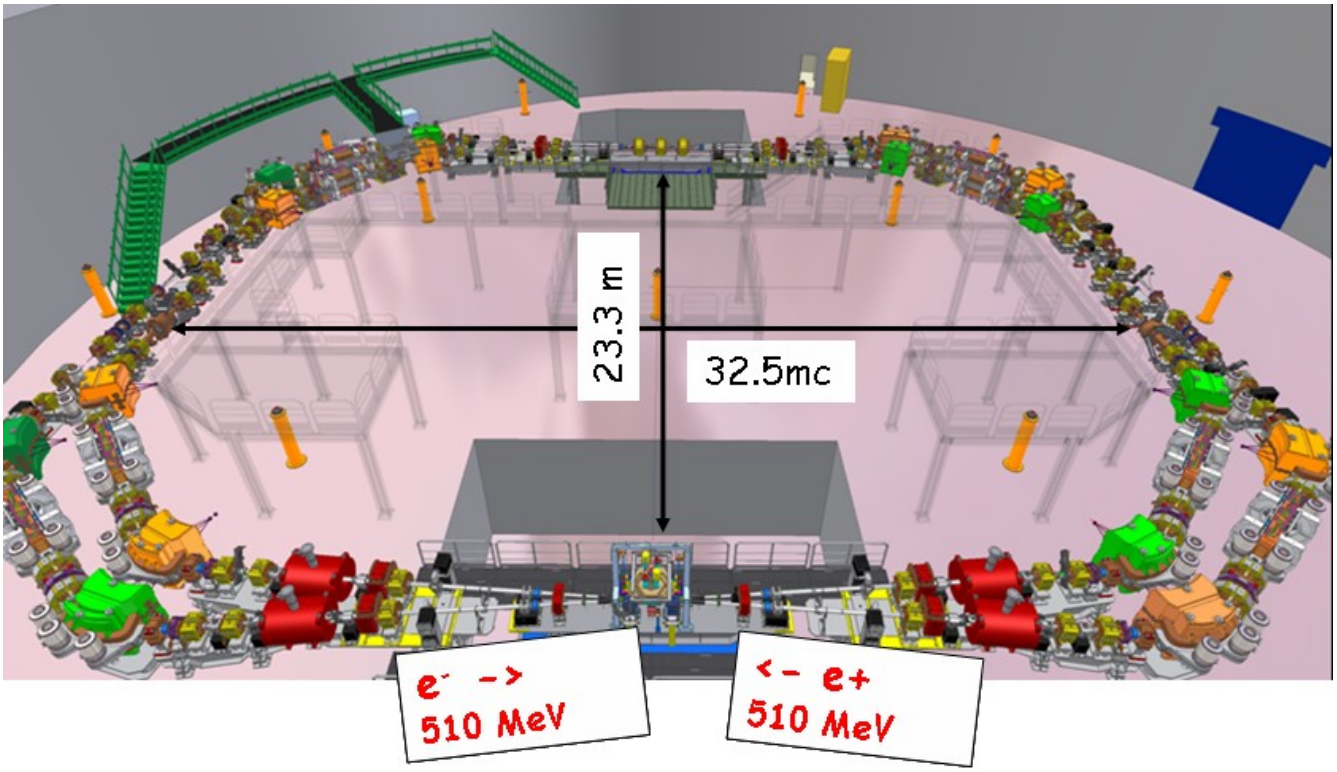

Figure 5.5 Overall view of the DAFNE collider

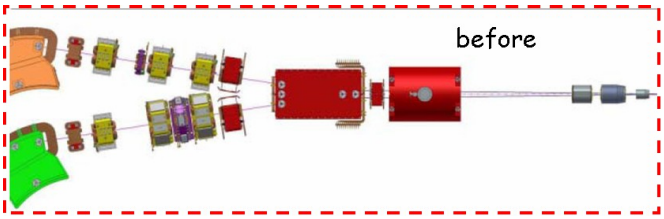

Figure 5.6 DAFNE's interaction region before the upgrade.

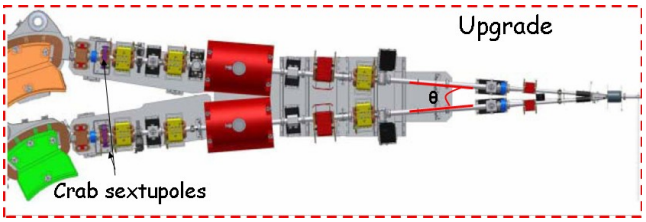

Upgraded DAFNE's interaction region. We can see that two beampipe instead of one before lead the electrons and positrons to the interaction point to allow a crossing angle. The arrows indicate the sextuples implementing the crab waists, located 9 meters away from the IP.

When those ones cross the scintillating tiles they deposit a part of their energy, which is converted into scintillation photons. These latter are collected by fibers glued on the surface of the tile, that drive them to a photo multiplier (PM). The higher the energy deposit, the higher the number of scintillating photons fund in the PM. Thus, the intensity of the light yield in the PM allows to derive the total energy of the incoming electron. The segmentation into modules and sectors also allows to check whether the electrons and positrons are produced back-to-back as expected in the case of BhaBha event. So, it helps to select signals event while rejecting background events. This procedure is made easier by the use of the GEM trackers.

On each side of the IP, the GEMs are made of 2 halfmoon-shaped halves, located above and below the beampipe, respectively. Each half is segmented into 8 azimuthal sectors and 4 radial rings, all of equal angular extent. This adds up to 32 cells. This finer segmentation provides additional information on the particles trajectory. Each cell is filled with a gas that is ionized when an electron or positron flies through it. The corresponding created charges are amplified by a high voltage set between the entry and exit faces of the GEM. This leads to an avalanche that is collected on a pad related to the electronic readout. The detection of a current in a pad signals that the corresponding cell has been hit by a particle.

Finally, two photon detectors are located 170 cm away from the IP. Their made of four scintillating crystals. As in the case of the tiles of the Calorimeters, when a particle crosses one of these detectors, it deposits energy that excites the crystal, and is converted into scintillation photons. Each of the 4 crystals is connected to a PM that detects these photons. Again, the photon yield allows to estimate the energy deposit. The primary role of these detectors is to detect photons emitted at low angle by radiative bhabhas. This provides an additional luminosity measurement, independent from that performed with the calorimeters and GEMs. Moreover, because the rate at which radiative bhabhas events occur at low angle is very high, it can be used to monitor the luminosity online : when DAFNE's physicist modify the setting of the collider the luminosity, they can immediately check the effect on the luminosity.

6. Background study

6.1 Detectors

In principles, the detectors described in section 5 can also be used to study the backgrounds. However, since the priority is to measure the luminosity as precisely as possible, the Calorimeters and GEMs are protected by lead walls meant to stop the background particles in order to get a Bhabha sample as pure as possible (see figure 5.1). Thus, these detectors are for the moment not relevant to study the backgrounds. On the other hand the photon detectors can be used. As can be seen on figure 6.1, they are also surrounded by lead bricks and can be hit only by particles going through a cylindrical window. By default, this window is aligned with the nominal trajectory of the photons emitted by radiative bhabhas, but it can be moved so that only particles from the background hit the detector.

Using the photon detectors, we can measure mainly two quantities. The first one is the rate at which it is hit by background particles, proportional to the total rate of background particles. The second one is the energy of these particles. Both quantities can be compared with the prediction of the simulations to check whether these latter are accurate and try to correct them if they're not.

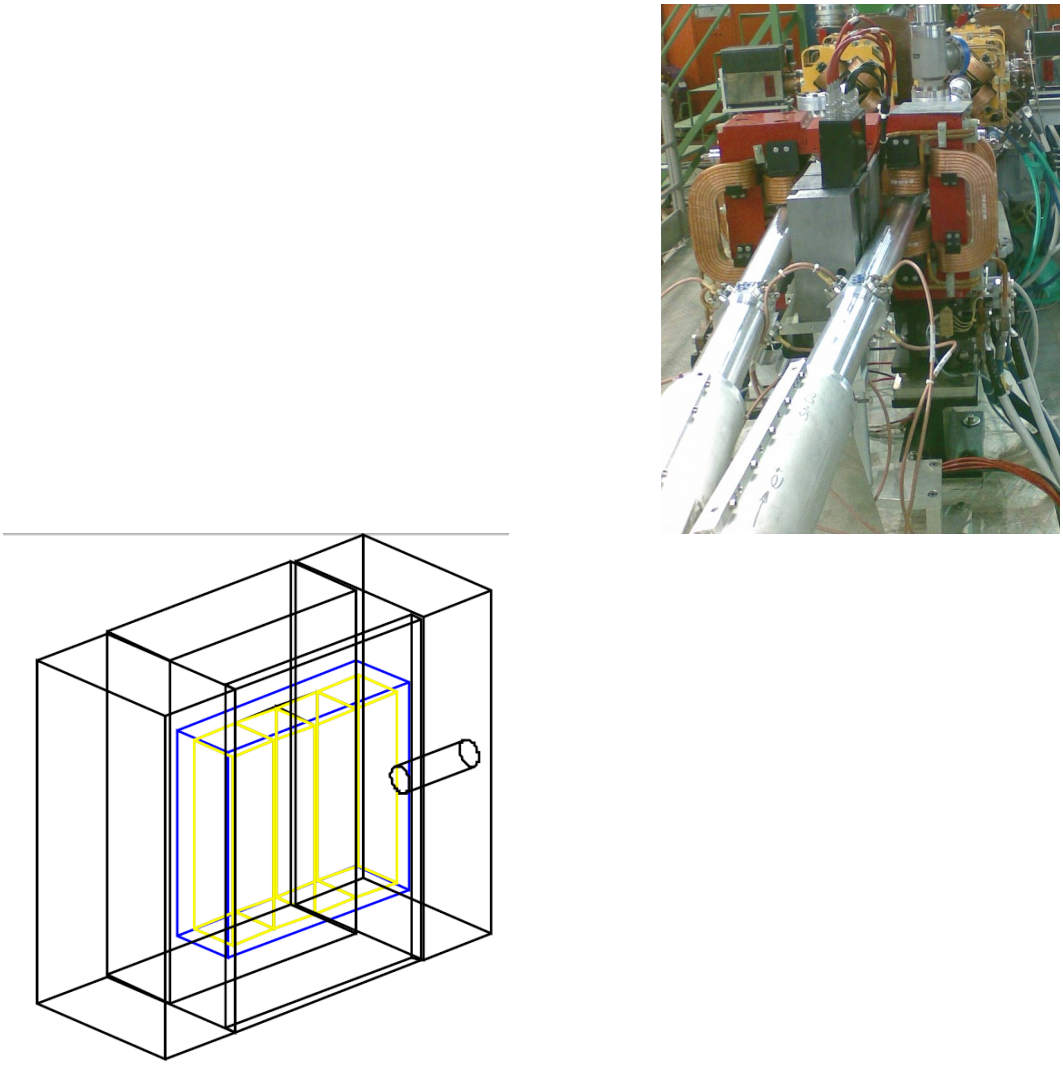

Fig.6.1. Right: photon detector installed in the interaction region. Left: photon detector in the preliminary GEANT-3 simulation.

6.1 Monte Carlo Simulation

A simulation predicting the rate and energy of the Touschek background particles, as well as the position where they leave the volume of the beampipe, has been developed by experts of the DAFNE collider []. It can not be used as such for a comparison with real data since it does not include the interaction between these particles and the various materials present in the interaction region, nor the response of the detectors. My work is to include this missing part, by developing a simulation based on the GEANT4 software. The final goal is to provide the prediction of the simulation for the background particles rate and the energy distribution of these particles, the two main quantities to be compared with real data.

Geant4 is a toolkit for the simulation of the passage of particles through matter. It can be used to define the geometry of an object, the material is it made of, and to simulate the physical processes occurring when a particle passed through it: energy deposit and/or decay into other particles. The effects of potential magnetic fields are also calculated.

The GEANT4 is an object-oriented software. To each physical object or process corresponds a C++ class. Typically, the user will first use classes that describe the geometry of the pieces of detectors he needs to simulate, and then the classes describing the properties various involved materials. Some other classes describe the magnetic fields, as well as the particles positions and momentum.

Following this scheme, I will first simulate the geometry outlined on figure 5.3: various sections of the beampipe, filled with vacuum, quadrupoles, lead walls and photon detectors. The GEMs and Calorimeters are not essential for this study. Thus, they will not be included in the first place. They might be included later on, to be sure that the material distribution in the interaction region is described accurately enough. Then the type of material will be specified for each component, and the quadrupoles magnetic fields implemented. Finally, we'll write the part that gets the particle tracking information to transform the energy deposits in the four crystals of the photon detectors into the number of scintillating photons collected by the PMs.

The next step will be to get a physical input by interfacing our simulation with the Touschek simulation mentioned above []. This simulation provides the state vector of the Touschek particle at the first position where they leave the beampipe, right outside this latter. To take into account their interaction with the materials, they have to be extrapolated back inside the beampipe. To do so easily, we'll use the following trick: we'll change the momenta of the tracks into their opposite and let GEANT track them into a "mirror detector" in which all materials are replaced by vacuum, and in which the vacuum inside the beampipe is replaced by some lead. This way, as soon as the particle reaches the inside of the beampipe, GEANT tracking will find a hit in the lead, that we can use to determine easily the position where the particle was just before it left the beampipe. Finally, objects of the class representing the particles will be created, filled with the state vector of the particles and this position, and store in a Root Ntuple [].

The last step of the simulation will be to use the ntuple created above as an input to the simulation and let GEANT calculate their interaction in the various material and the energy deposit in the photon detectors. From this, we'll derive the background hits rate and the energy distribution of the background particles.